

Can natural variability explain the discrepancy between observed and modeled sea ice trends?

ERICA ROSENBLUM* AND IAN EISENMAN

Scripps Institution of Oceanography, University of California at San Diego, La Jolla, CA, USA

ABSTRACT

Observations indicate that the Arctic sea ice cover is rapidly retreating while the Antarctic sea ice cover is steadily expanding. State-of-the-art climate models, by contrast, tend to predict a moderate decrease in both the Arctic and Antarctic sea ice covers. A number of recent studies have attributed this discrepancy in each hemisphere to natural variability, suggesting that the models are consistent with the observations when simulated natural variability is taken into account. Here we examine sea ice changes during 1979–2013 in simulations from the most recent Coupled Model Intercomparison Project (CMIP5) as well as the Community Earth System Model Large Ensemble (CESM-LE). We find that accurately simulated Arctic sea ice retreat occurs only in simulations with too much global warming, whereas accurately simulated Antarctic sea ice expansion tends to occur in simulations with too little global warming. We show that because of this, simulations from both ensembles do not capture the observed asymmetry between Arctic and Antarctic sea ice trends. Using two separate methods to account for biases in the level of global warming in each simulation, we find that both ensembles imply that Arctic sea ice retreat as fast as observed would occur less than 1% of the time due to natural variability alone, and that Antarctic sea ice expansion as fast as observed would occur less than about 3% of the time. This suggests that there are systematic biases in current climate models in both polar regions.

1. Introduction

In comprehensive climate model simulations of long-term climate change, individual models are often used to carry out multiple simulations that differ only in their initial conditions. The spread among the simulations represents a range of possible realizations of natural variability in the climate system. Therefore an individual simulation would not typically match the observations on decadal timescales even if the model were perfect, but the observations are expected to fall within the range of the ensemble of simulations.

Modeling groups from around the world have contributed to each phase of the Coupled Model Intercomparison Project (CMIP). In the previous phase, CMIP3 (Meehl et al. 2007), Stroeve et al. (2007) found that virtually none of the models simulated a summer Arctic sea ice cover that diminished as fast as in the observations. Overall the models simulated sea ice trends that were more consistent with observations in the Antarctic than in the Arctic (Stroeve et al. 2007; IPCC 2007). However, because of the limited number of CMIP3 simulations, Stroeve et al. (2007) suggested that the observed Arctic sea ice retreat

may represent a rare realization of natural variability that would therefore be captured in only a small fraction of the simulations.

The observed Arctic sea ice trend is better simulated in the current phase (Stroeve et al. 2012; IPCC 2013), CMIP5 (Taylor et al. 2011). We analyze the cause of this improvement in a companion paper (Rosenblum and Eisenman 2016). This is a newer generation of comprehensive climate models and includes more simulations from many of the models. The ensemble mean in CMIP5 still underestimates the observed Arctic sea ice retreat (Stroeve et al. 2012; IPCC 2013), but the observations now fall comfortably within the range of simulations (Figures 1b,e). Therefore, many recent studies have suggested that the observed Arctic sea ice trend is accurately captured by the models when simulated natural variability is accounted for (Swart et al. 2015; Notz 2014; Stroeve et al. 2012; IPCC 2013; Kay et al. 2011; Holland et al. 2008). This would imply that global warming is causing some of the observed Arctic sea ice retreat, and that it is enhanced by decadal-scale natural variability.

During the past several years, there was a notable emergence of a statistically significant positive observed sea ice trend in the Antarctic (Eisenman et al. 2014). Most CMIP5 models are unable to simulate this trend (Figures 1c,f) (e.g., Turner et al. 2013; Zunz et al. 2013; IPCC

*Corresponding author address: Scripps Institution of Oceanography, University of California at San Diego, La Jolla, CA, USA.
E-mail: ejrosenb@ucsd.edu

2013), contributing to a consensus view that there is “low confidence” in the scientific understanding of the observed Antarctic sea ice expansion (IPCC 2013). Nonetheless, a number of recent studies have argued that the models are still at least marginally consistent with observations when the range of natural variability is considered (Turner et al. 2013; Swart and Fyfe 2013; Zunz et al. 2013; Mahlstein et al. 2013; Polvani and Smith 2013; Goosse and Zunz 2014; Gagné et al. 2014; Fan et al. 2014; Purich et al. 2016; Ice et al. 2015). In this view, natural variability in the Antarctic has overwhelmed the ice retreat that would occur due to global warming to allow the observed increase in the sea ice cover.

Consequently, these recent studies suggest that natural variability rectifies the differences between typical state-of-the-art climate model simulations and observed Arctic and Antarctic sea ice trends. However, anthropogenic forcing affects sea ice trends through many physical processes, some of which may not be well simulated in current models (e.g., Bintanja et al. 2013; Zunz et al. 2013; Mahlstein and Knutti 2012; Mahlstein et al. 2013; Jahn et al. 2012; Haumann et al. 2014; Uotila et al. 2014; Purich et al. 2016; Rampal et al. 2011). This allows the possibility that models may simulate sea ice trends that are consistent with observations for the wrong reasons.

Here we consider one such possibility related to simulated biases in the level of global warming (Figure 1a,d). We examine all available CMIP5 simulations of years 1979–2013. There are 37 different climate models, many of which submitted multiple simulations, leading to a total of 100 ensemble members. Therefore, the CMIP5 ensemble members differ due to both inter-model differences and natural variability.

In order to isolate the influence of natural variability alone, we also consider simulations from the Community Earth System Model Large Ensemble (CESM-LE) (Kay et al. 2014), which includes 30 ensemble members that are all generated with the same model and differ only in initial conditions. See Table S1 for a list of models and Appendix A for further details.

Some previous studies have focused on the September or March sea ice trend, whereas others have considered the annual mean. Here we focus on annual-mean trends, thereby averaging over seasonal variability that may be unrelated to long-term trends. For an analysis of September Arctic sea ice trends, see Rosenblum and Eisenman (2016).

2. Observed and simulated sea ice trends

As a starting point, we consider the extent to which the observations lie within the distribution of CMIP5 simulated 1979–2013 Arctic and Antarctic sea ice trends. If we assume that these distributions are well sampled, then each distribution represents the range of sea ice trends allowed

by natural variability and differences in model physics. Examining each hemisphere individually, we find that in both cases the observed sea ice trend lands within the distribution of CMIP5 simulations (Figure 1e–f).

To quantify the level of agreement, we determine the number of simulated trends that are at least as far in the tail of the CMIP5 distribution as the observed trend. We find that 16 of the 100 simulations have Arctic sea ice retreat as fast as the observations and 3 of the 100 simulations have Antarctic sea ice expansion as fast as the observations (Table 1). This implies that if the CMIP5 models are correct, then the probability that the Arctic sea ice would retreat as fast as observed is 16%, and the probability that the Antarctic sea ice would expand as fast as observed is 3%. These results are similar to previous studies that found that models and observations are consistent when accounting for simulated natural variability in the Arctic (Swart et al. 2015; Notz 2014; Stroeve et al. 2012) and perhaps marginally consistent in the Antarctic (Swart and Fyfe 2013; Turner et al. 2013; Zunz et al. 2013; Purich et al. 2016).

We also use Gaussian fits of the distributions as an alternative method of assessing the level of agreement. This will be useful later in the analysis when the observations fall in the tail of the distributions. Such a fit is accurate, for example, if we treat all simulations as realizations from the same ensemble and assume that the simulated sea ice retreat is a linear trend with superimposed natural variability that takes form of white noise. Under this construction, the center of the distribution is often considered to be the response to external forcing, and the width of the distribution indicates the influence of natural variability. Using this method, we find that 14% of runs in the Gaussian distribution have Arctic sea ice retreat at least as fast as the observations and 1.6% of runs have Antarctic sea ice expansion as fast as the observations, similar to the values found with the first method above.

3. Sea ice scales with global temperature

If accurate Arctic sea ice retreat is only simulated in runs that have far too much global warming, then this suggests that the models may be getting the right Arctic sea ice retreat for the wrong reasons. Similar considerations apply if a model simulates an accurate Antarctic sea ice trend but too little global warming. This concern is noteworthy for the Arctic because the models tend to simulate too large a rate of global warming during 1979–2013 (Figure 1a,d) (note that this bias depends on the specific time period). Further, we find that Arctic sea ice extent and global-mean surface air temperature are approximately linearly related in most of these models (Figure S1a). The two quantities have an average correlation of -0.94 in the CMIP5 simulations of 1900–2100 that we analyze (see Appendix A for details) and a correlation of

-0.99 in the CESM-LE simulations of 1920-2100 (Figure S1c,e). This result is similar to previous studies that have discussed the close and approximately linear nature of this relationship (Gregory et al. 2002; Winton 2011; Mahlstein and Knutti 2012; Stroeve and Notz 2015). In the Antarctic, we find that sea ice extent and global-mean surface air temperature have a somewhat smaller average correlation of -0.86 and -0.98 in the CMIP5 and CESM-LE simulations, respectively (Figure S1d,f).

This tight relationship implies that biases in global-mean surface temperature trends may be directly related to biases in sea ice trends in both hemispheres (cf. Winton 2011). To assess whether this is occurring in simulations of 1979-2013, we plot the Arctic and Antarctic sea ice trend in each CMIP5 simulation versus the simulated trend in global-mean surface air temperature (Figure 2a-b). A relationship is visually apparent, implying that much of the inter-model variation in the sea ice trends is associated with differences in the level of simulated global warming. That is, simulations with large global warming trends have more sea ice retreat. We find that all of the simulations with Arctic sea ice trends that fall near the observations have global warming trends that are approximately 1.4-2.1 times larger than the observed trend (Figure 2a). Similarly, each simulation with a temperature trend similar to the observations underestimates the Arctic sea ice retreat by at least 30%. By contrast, runs with approximately accurate levels of global warming tend to land closer to the observed Antarctic sea ice trend, although they still tend to simulate Antarctic sea ice retreat rather than the observed expansion (Figure 2b).

We remove inter-model differences from this analysis by considering the CESM-LE simulations of 1979-2013 (Figure 3a-b). Here we find an even stronger relationship between the trend in global-mean surface temperature and the trend in Arctic or Antarctic sea ice cover (correlations of -0.73 and -0.81 in the Arctic and Antarctic, respectively). This illustrates that the relationship between sea ice changes and the level of global warming remains fairly constant from one simulation to another within a single model, similar to Winton (2011) who examined the evolution of this relationship over 1979-2100 in several CMIP3 models.

As a result, we find that the relationship between global warming and sea ice trends can arise solely from simulated natural variability that does not involve inter-model differences in climate sensitivity. In other words, realizations of natural variability that have anomalously large levels of global warming during 1979-2013 also tend to have anomalously large levels of sea ice retreat in both hemispheres (see example in Figure S2). This is consistent with Xie et al. (2016), who found that simulated natural variability in global-mean temperature projects substantially onto both polar regions.

4. Arctic-Antarctic asymmetry

Given that the global-mean surface air temperature trends appear to be related to both Arctic and Antarctic sea ice trends in climate models, we examine whether simulations of 1979-2013 capture the asymmetric sea ice trends found in observations. By indicating the extent to which each simulation over- or under-predicts the global-mean surface temperature trend, Figure 4a illustrates that the CMIP5 models are largely unable to simulate the asymmetric sea ice trends found in observations. In general, a sea ice trend in one hemisphere may be accurately simulated only at the expense of accuracy in the other. Further, the accurate hemisphere requires an inaccurate temperature trend. That is, simulations that warm too rapidly compared to observations are more likely to accurately predict Arctic sea ice trends but to simulate too much sea ice retreat in the Antarctic. The reverse also appears to be true, although there are far fewer simulations in CMIP5 that underestimate global warming trends.

We repeat this analysis using CESM-LE simulations to remove inter-model differences. Figure 4b demonstrates that this result is at least partly due to natural variability alone. This raises questions regarding whether wind and pressure anomalies are strongly impacting the distribution of sea ice trends allowed by natural variability in this model, as was suggested in previous studies (Wettstein and Deser 2014), because such atmospheric anomalies would not typically be expected to be correlated between the Arctic and Antarctic such that they similarly impact the sea ice trends in both hemispheres.

5. Effective sea ice trend

These results demonstrate that global-mean surface air temperature trends appear to be directly related to both Arctic and Antarctic sea ice trends in these climate models. Here we consider a simple method to account for biases in the level of simulated global warming that leverages the approximate linearity between sea ice extent and global-mean surface air temperature (Figure S1). Using the approximation that the proportionality between trends in sea ice extent and global temperature in each simulation does not depend on the level of global warming (which would hold if this relationship were perfectly linear), we can scale the sea ice trend in each simulation to approximately account for the bias in global warming:

$$\left(\frac{dI}{dt}\right)_{\text{eff}} \equiv \left(\frac{dI}{dt} / \frac{dT}{dt}\right)_{\text{sim}} \left(\frac{dT}{dt}\right)_{\text{obs}}. \quad (1)$$

We define the term on the left-hand side as the “effective sea ice trend”, which is meant to approximate what the value of the simulated sea ice trend would have been if the model had accurately captured the observed level of global warming. The quotient on the right-hand side is

the simulated change in sea ice extent per degree of global warming (measured in km^2/K), which is an estimate of the “sea ice sensitivity” based on the ratio of temporal trends (Winton 2011). The ice sensitivity is then scaled by the observed global-mean surface temperature trend, which is the final term on the right-hand side.

Using the effective sea ice trend causes the result presented in Section 2 to change substantially (compare red and blue confidence intervals in Figure 2c-d). First, the ensemble-mean predicted sea ice retreat becomes slower in each hemisphere by more than 35%, consistent with the above result that sea ice trends associated with the observed level of global warming tend to be smaller than the average simulated sea ice trends (Section 3 and Figure 2a-b). This implies that the sea ice response to external forcing is expected to be smaller when scaled to the observed level of global warming. Second, the width of the simulated sea ice trend distribution decreases, implying that, for a given temperature trend, there is a much narrower distribution of sea ice trends that can arise due to natural variability: the standard deviation of each distribution decreases by 35-40%. As a result, we find that 0 of the 100 CMIP5 simulations have an Arctic effective sea ice retreat as fast as the observations. Similarly, 0 of the 100 CMIP5 simulations have an Antarctic effective sea ice expansion as large as the observations (Table 1).

Fitting a Gaussian to the distributions to approximately estimate values for the tails that are not sufficiently populated by the 100 members, we find that the percentage of runs in the Gaussian distribution that have Arctic sea ice retreat as fast as the observations drops from 14% (Figure 1e) to 0.08% (Figure 2c). In the Antarctic, biases in the level of global warming appear to have a somewhat smaller effect. Although the center of the Antarctic distribution moves closer to the observed value, the width of the distribution decreases sufficiently to cause the percentage of runs in the distribution that have Antarctic sea ice expansion as large as the observations to drop from 1.6% (Figure 1f) to 0.42% (Figure 2d). Note that this result is qualitatively consistent with the Antarctic sea ice sensitivities reported by Purich et al. (2016).

It is noteworthy that the discrepancies between the models and observations have similar magnitudes in the Antarctic as the Arctic when using effective sea ice trends (Figure 2c-d). This is in contrast to the analysis of sea ice trends, where the bias was larger in the Antarctic (Figure 1e-f).

We repeat this analysis using CESM-LE simulations of 1979-2013 and find similar results (Figure 3c-d). Overall, the results of this section imply that the possibility that natural variability alone could explain the difference between the observed and modeled sea ice trends in either hemisphere decreases substantially after accounting for biases in the level of global warming.

6. Pseudo-ensemble from longer time period

Next, we explore an alternative method to estimate the distribution of simulated sea ice trends that would emerge under the observed level of global warming. Specifically, we assume that the relationship between global warming and sea ice changes is the same for any 35-year time period (which would hold if the relationship between sea ice extent and global-mean temperature were perfectly linear). We therefore examine the trends during all overlapping 35-year periods in each of the CMIP5 simulations of 1900-2100 (see Appendix A for details). Figure 5a-b shows each of the 12,024 overlapping 35-year trends in annual-mean global-mean surface air temperature and sea ice extent. The 1979-2013 trends are also shown in red, illustrating the qualitatively similar relationship between trends in sea ice and global temperature during this and other 35-year periods.

To validate this method, we consider the distribution of sea ice trends during all 35-year periods that have levels of global warming similar to the simulated 1979-2013 distribution (i.e., similar to Figure 1d). Specifically, we select all the 35-year periods during 1900-2100 that have temperature trends within one standard deviation of the 1979-2013 ensemble mean (red shaded region in Figure S3a,b) and examine the corresponding histogram of sea ice trends (Figure S3c,d). We find that this distribution of 3,581 sea ice trends (Figure S3c,d) closely matches smaller distribution of simulated sea ice trends during 1979-2013 (Figure 1e,f): the red and black error bars in Figure S3c,d are closely aligned. This implies that this method allows us to build a far larger “pseudo-ensemble” that approximately represents 1979-2013 by harvesting time periods with similar levels of global warming from the 200-year simulations.

Motivated by this, we create a pseudo-ensemble of periods in the simulations that have global warming trends similar to the 1979-2013 observed value. This provides an approximation of the spread of simulated sea ice trends that would coincide with the observed level of global warming. Each simulated 35-year global warming trend that is similar to the observations (i.e., within the 68% linear regression confidence interval of the observed trend after accounting for autocorrelation; see Appendix C for details) is highlighted in green in Figure 5a-b. Here the pseudo-ensemble is comprised of the distribution of 1,251 35-year periods that fall within this green shaded region (Figure 5c,d).

Only 1 (0.08%) of the 1,251 sea ice trends from this pseudo-ensemble has an Arctic sea ice retreat that is as large as the observations (Table 1). Therefore, this analysis of years 1900-2100 in the simulations yields a similar result to the analysis in Section 5 using 1979-2013 effective sea ice trends. This is consistent with our finding that the pseudo-ensemble distribution (Figure 5c) is fairly sim-

ilar to the distribution of effective sea ice trends (Figure 2c), which can be seen by comparing the black and blue confidence intervals in Figure 5c.

Additionally, analogous to the comparison of the effective sea ice trend distribution with the sea ice trend distribution in Section 5, here we compare the pseudo-ensemble associated with the observed 1979-2013 level of global warming (Figure 5c) with the pseudo-ensemble associated with the ensemble of simulated 1979-2013 levels of global warming (Figure S3c). The results are broadly similar. First, 7.8% of the Arctic sea ice trends from Figure S3c are at least as negative as the observed value, compared to 0.08% in Figure 5c. Second, the pseudo-ensemble mean associated with too much global warming (Figure S3c) is approximately 23% larger than the pseudo-ensemble mean associated with the observed level of global warming (Figure 5c).

We find some qualitative similarities in the results for the Antarctic. First, the Antarctic pseudo-ensemble and effective sea ice distribution are qualitatively similar (compare error bars in Figure 5d). Second, the pseudo-ensemble mean associated with the observed level of global warming (Figure 5d) is about 40% smaller than the pseudo-ensemble mean associated with the simulated level of global warming (Figure S3d). Yet, 2.6% of the 35-year periods from the pseudo-ensemble associated with the 1979-2013 observed warming have Antarctic sea ice expansion as large as the observations (Table 1, Figure 5d), compared to 1.5% of the 35-year periods from the pseudo-ensemble associated with the 1979-2013 simulated warming (Figure S3d). This is in contrast with the effective sea ice trend results in Section 5. The reason may be related to the assumption of a temporally constant ice sensitivity applying better in the Arctic than in the Antarctic. For example, in Figures S1b, the Antarctic sea ice sensitivity in CESM-LE is larger during 1900-2000 (bottom right part of plot: small warming leads to large ice retreat) than during 2001-2100 (remainder of plot: more gradual ice retreat during continued warming). This may be associated with the Antarctic sea ice sensitivity being influenced by ozone forcing in the Antarctic region, which does not scale with greenhouse forcing during 1900-2100. This and similar effects may cause the pseudo-ensemble approach, which assumes constant ice sensitivity during 1900-2100, to be less effective in the Antarctic than the Arctic.

7. Discussion

The analyses in Sections 5 and 6 rely on the assumption that the relationship between sea ice extent and global-mean surface air temperature is approximately linear. In the Arctic, simulated sea ice extent is highly correlated with global-mean surface air temperature (left column of Figure S1). This tight relationship is consistent with the previous finding that the Arctic sea ice sensitivity in a

given model does not depend on the forcing scenario (Winton 2011).

While the same is not true of the Antarctic sea ice extent, which is not as strongly correlated with global-mean surface air temperature (right column of Figure S1), the distributions in Figures 2b, 3b, and 5b suggest that the correlations between Antarctic sea ice extent and global-mean surface air temperature may be large enough that the relationship between the trends of these two values during 35-year periods are directly related, causing simulated Antarctic sea ice expansion to occur more often in simulations with too little global warming.

These results are relevant to previous studies that used control simulations with constant forcing to determine whether the observed trends can be explained by natural variability alone (Kay et al. 2011; Polvani and Smith 2013; Mahlstein et al. 2013). For example, Polvani and Smith (2013) point out that Antarctic sea ice trends that are up to three times as large as the observed trend can naturally emerge in control simulations. They suggest that this implies that the natural variability of this system is large enough to overwhelm the forced global warming signal, similar to arguments made by Mahlstein et al. (2013). However, the results presented here imply that periods in control simulations with expanding Antarctic sea ice are likely to have global warming trends that are significantly below the 1979-2013 observed trend (IPCC 2013). Therefore, these results imply that when simulated global warming trends are not considered, neither the center nor the width of the distribution of sea ice trends in a control simulation should be expected to accurately reflect the range of possible sea ice trends that can emerge in climate models under the observed level of global warming.

The results presented here stem from the point that the observed relationship between sea ice extent and global-mean surface temperature, i.e., the observed sea ice sensitivity, is markedly different in each hemisphere from that simulated by climate models. It should be emphasized that the physical process that determine the ice sensitivity are not well understood. Therefore, this bias may be related to issues in the atmosphere, ocean, or sea ice components of the models that are connected to the simulated sea ice changes or the level of global warming. A number of studies have identified model biases that may impact sea ice trends (Bintanja et al. 2013; Zunz et al. 2013; Mahlstein and Knutti 2012; Mahlstein et al. 2013; Jahn et al. 2012; Haumann et al. 2014; Uotila et al. 2014; Purich et al. 2016; Rampal et al. 2011) or global warming trends (e.g., IPCC 2013; Kosaka and Xie 2013).

Note that an analysis of the sea ice sensitivity in CMIP5 was also recently presented by Stroeve and Notz (2015), who found good agreement with observations, in contrast with the results presented here. The source of this difference is discussed in Rosenblum and Eisenman (2016).

We have examined the sensitivity of these results to adjustments in various aspects of the methodology. First, the results presented here use sea ice extent as a measure of the sea ice cover. The influence of switching to sea ice area in the models and observations is discussed in Appendix B. Second, in the analysis above, each run has been treated for simplicity as a realization from a single ensemble, as if all runs were generated by the same model. Alternatively, each run could be treated as a realization from a separate ensemble, as if all runs were generated by different models, following Stroeve et al. (2012) and Santer et al. (2008). We repeat the analyses in Sections 2 and 5 using this framework in Appendix C. Third, we carry out a more complicated pseudo-ensemble approach that more accurately captures the target distribution in Appendix D. Fourth, in Appendix E we repeat the effective sea ice trend analysis (Section 5) but compute the sea ice sensitivity in Eq. (1) using a total least squares regression rather than the ratio of ice and temperature temporal trends. In each case, consistent with our main results, we find that after accounting for biases in the level of global warming, (1) the possibility that natural variability can explain the difference between the models and the observations becomes exceedingly small and (2) there is a similar disagreement between the models and the observations in the two hemispheres.

8. Conclusion

In each hemisphere, the observed 1979-2013 trend in sea ice extent falls at least marginally within the distribution of the CMIP5 simulations (Figure 1b,c,e,f). Consistent with this, a number of previous studies have suggested that natural variability can explain the discrepancy between the observed sea ice trend and the ensemble-mean simulated trend in each hemisphere (Swart et al. 2015; Notz 2014; Stroeve et al. 2012; Turner et al. 2013; Swart and Fyfe 2013; Zunz et al. 2013; Kay et al. 2011; Polvani and Smith 2013; Mahlstein et al. 2013; Gagné et al. 2014; Holland et al. 2008; Goosse and Zunz 2014; IPCC 2013; Fan et al. 2014; Purich et al. 2016).

The results presented here suggest that this viewpoint breaks down when we account for biases in global-mean surface temperature trends: model runs with accurate Arctic sea ice trends all have too much global warming, whereas periods with accurate Antarctic sea ice trends tend to have too little global warming. Relatedly, the models are not able to simulate the asymmetric sea ice trends found in the observations. Hence the results suggest that the difference between observed and modeled sea ice trends in each hemisphere cannot be attributed to simulated natural variability alone. This implies systematic errors in the Arctic and Antarctic sea ice changes simulated with current models (e.g., Bintanja et al. 2013; Zunz et al. 2013; Mahlstein and Knutti 2012; Mahlstein et al.

2013; Jahn et al. 2012; Haumann et al. 2014; Uotila et al. 2014; Purich et al. 2016; Rampal et al. 2011), or possibly errors in the observations (e.g., Eisenman et al. 2014; Karl et al. 2015; Screen 2011).

Acknowledgments. The work was supported a National Science Foundation Graduate Research Fellowship and National Science Foundation grants ARC-1107795 and OCE-1357078.

APPENDIX A

Methods

Here further details are given regarding the observations and the processing of the CMIP5 model output.

For the observed monthly-mean sea ice extent and sea ice area, we use the National Snow and Ice Center Sea Ice Index (Fetterer et al. 2002), which uses the NASA Team algorithm to estimate sea ice concentration from passive microwave satellite measurements. Missing values are filled by interpolation between the same months in the previous and following years. We use the Goddard Institute for Space Sciences Surface Temperature Analysis (GISSTemp) (Hansen et al. 2010) for the observed annual-mean global-mean surface temperature data.

We analyze 100 simulations of years 1979-2013 from 37 CMIP5 models, using the Historical (1850-2005) and RCP4.5 (2006-2100) experiments. The models simulate surface air temperatures at each horizontal atmospheric grid point, and sea ice concentration is typically simulated on the ocean grid. Therefore, the areas of the cells in both grids are needed to compute the total Arctic and Antarctic sea ice areas as well as the global-mean temperature. The following models did not have grid cell areas reported in the CMIP5 archive: CanCM4 (surface air temperature), MPI-ESM-LR (surface air temperature), FIO-ESM (surface air temperature and sea ice). In these cases, grid cell areas were estimated from the reported locations of grid cell corners using the Haversine formula (note that this formula could only be used with regular grids).

Simulations were not used in this study when either surface air temperature output was not available during all of 1979-2013, sea ice output was not available during all of 1979-2013, dates reported in the file did not match the filename in the CMIP5 archive, Historical simulation parent files for RCP4.5 simulations were not reported, irregular grids were used but grid cell areas were not provided, or latitudinal bounds exceeded 90 degrees. The following runs each had at least one of these issues and hence were excluded: EC-EARTH runs 1,3,5,6,10; FIO-ESM run 2; MIROC-ESM-CHEM run 2; CESM1-CAM5-1-FV2 runs 1-4; GFDL-CM3 runs 3 and 5; GFDL-CMP2p1 runs 1-10; all runs from the HadGEM models; all runs from BCC-CSM1-1-M; all runs from INMCM; and CanESM2 run 1.

GFDL-ESM2G run 1 also excluded because the Antarctic sea ice extent gradually decreases and then increases during 1979-2013, leading to a highly autocorrelated time series of linear regression residuals with less than 2 effective degrees of freedom, which causes the standard error in the analysis in Appendix C to be complex (cf. eq. (4) in Santer et al. 2008). Additional simulations were excluded from the analysis in Figure 5 because data was not available for the entire 1900-2100 period. Additionally, EC-EARTH runs 5-8 were excluded because the dates in the sea ice concentration files did not match the dates in the surface air temperature files.

APPENDIX B

Using ice area instead of ice extent

The results presented in the main text use sea ice extent as a measure of the sea ice cover. Here we briefly summarize the effect of instead using sea ice area in the models and observations. First, considering the Gaussian distribution of sea ice trends (as in Figure 1e-f), we find that 12% of the simulations would have Arctic sea ice retreat that is as large as the observations, and 1.5% would have Antarctic sea ice expansion as large as the observations, similar to the values of 14% and 1.6%, respectively, that we found for ice extent. These values drop to 0.02% and 0.30% (similar to 0.08% and 0.42% for ice extent), respectively, when we use the Gaussian distribution of Arctic and Antarctic effective sea ice trends (as in Figure 2c-d). Lastly, of the 1,251 overlapping 35-year periods that have global warming trends that are similar to the 1979-2013 observations (as in Figure 5c-d), 2 periods have Arctic sea ice trends as negative as the observed value, and 27 periods have Antarctic sea ice trends as positive as the observed value (similar to 1 and 32, respectively, for ice extent).

APPENDIX C

Paired Trend Analysis

In this section, we consider an alternative framework for the analysis in the main text: rather than treat each CMIP5 simulation as a realization from a single model, here we treat each simulation as a realization from a separate model. Following previous studies (Stroeve et al. 2012; Santer et al. 2008), we determine if each simulated trend is statistically different from the observed trend at the 95% confidence level by using Welch's t-test statistic:

$$d = \frac{\beta_m - \beta_o}{\sqrt{\sigma_m^2 + \sigma_o^2}}. \quad (C1)$$

Here β_m and β_o are the modeled and observed trends, respectively, and σ_m and σ_o are the associated standard errors, which are adjusted for autocorrelation following Santer et al. (2008). A value of $|d| > 1.96$ is equivalent to zero falling outside of the 95% confidence interval of a Gaussian distribution with a mean of $\beta_m - \beta_o$ and a standard deviation of $\sqrt{\sigma_m^2 + \sigma_o^2}$. In Figure S4a-b, β_o and β_m are the observed and modeled sea ice trends, which are represented by a series solid black dots (one for each simulation). The standard errors, σ_o and σ_m , are also shown. In Figure S4c-d, β_m is the effective sea ice trend and σ_m is determined using error propagation:

$$\sigma_m = \sqrt{\left(\frac{\beta_m}{\beta_{I_i}} \sigma_{I_i}\right)^2 + \left(\frac{\beta_m}{\beta_{T_i}} \sigma_{T_i}\right)^2 + \left(\frac{\beta_m}{\beta_{T_i^o}} \sigma_{T_i^o}\right)^2}, \quad (C2)$$

where β_{I_i} , β_{T_i} , and $\beta_{T_i^o}$ are the trends in simulated sea ice, simulated global-mean surface temperature, and observed global-mean surface temperature, and σ_{I_i} , σ_{T_i} , and $\sigma_{T_i^o}$ are the associated standard errors.

We find that of the 100 simulations, 39% simulate sea ice trends that are statistically different from the observations at the 95% confidence level in the Arctic, and 81% in the Antarctic. On the other hand, 77% and 84% simulate Arctic and Antarctic effective sea ice trends that are statistically different from the observations.

APPENDIX D

Using scaled histograms in pseudo-ensemble analysis

In this appendix, we repeat the calculation in Section 6 (Figure 5a-b) using a somewhat more precise but less straightforward approach that involves a weighting function rather than simply selecting the runs that fall within the shaded region. We begin with the distribution of 12,024 overlapping 35-year temperature trends during 1900-2100 as well as a gaussian distribution centered on the observed temperature trend with a width equal to the 68% linear regression confidence interval (which is adjusted for autocorrelation, see Appendix C for details). Next, we assign each 35-year period a weight equal to the height of the gaussian at the center of the histogram bin of this 35-year period divided by the number of runs in the histogram bin.

These weights scale the distribution of temperature trends during 1900-2100 to match a distribution consistent with the observed 1979-2013 temperature trend. Next, we create a histogram of sea ice trends with each 35-year period multiplied by its weight. Hence this approach asks what range of ice extent trends is consistent with the observed temperature trend under the assumptions described in Section 6. We find that the resulting distribution is approximately equivalent to result of the simpler approach

in Section 6 (Figure 5c-d): 0.32% of the 35-year periods have Arctic sea ice trends are at least as negative as the observed value, and 3.9% have Antarctic sea ice trends at least as positive as the observed value, compared with 0.08% and 2.6%, respectively reported in Section 6.

APPENDIX E

Using total least squares to compute sea ice sensitivity

Winton (2011) found that computing the ice sensitivity using a total least squares (TLS) regression between ice extent and global-mean surface air temperature leads to a slightly more accurate estimate than the ratio of ice and temperature temporal trends as in Eq. (1). We find that replacing the ratio of trends in Eq. (1) with a TLS regression between ice extent and global-mean surface air temperature yields similar results: using Gaussian fits to the distributions, we find that the probability that the observations would land this far from the TLS effective sea ice trend ensemble mean is 0.06% in the Arctic and 0.10% in the Antarctic (similar to 0.08% and 0.42%, respectively, using the trend ratio).

References

- Bintanja, R., G. J. van Oldenborgh, S. S. Drijfhout, B. Wouters, and C. a. Katsman, 2013: Important role for ocean warming and increased ice-shelf melt in Antarctic sea-ice expansion. *Nature Geoscience*, **6** (5), 376–379, doi:10.1038/ngeo1767.
- Eisenman, I., W. N. Meier, and J. R. Norris, 2014: A spurious jump in the satellite record: has Antarctic sea ice expansion been overestimated? *The Cryosphere*, **8** (4), 1289–1296, doi:10.5194/tc-8-1289-2014.
- Fan, T., C. Deser, and D. P. Schneider, 2014: Recent Antarctic sea ice trends in the context of Southern Ocean surface climate variations since 1950. *Geophysical Research Letters*, **41** (7), 2419–2426, doi:10.1002/2014GL059239.
- Fetterer, F., K. Knowles, W. Meier, and M. Savoie, 2002: Sea ice index. *Natl. Snow and Ice Data Cent., Boulder, Colo.*, (Updated 2012.) <http://nsidc.org/data/g02135.html>.
- Gagné, M., N. P. Gillett, and J. C. Fyfe, 2014: Observed and simulated changes in Antarctic sea ice extent over the past 50 years. *Geophysical Research Letters*, doi:10.1002/2014GL062231.Abstract.
- Goosse, H., and V. Zunz, 2014: Decadal trends in the Antarctic sea ice extent ultimately controlled by ice-ocean feedback. *Cryosphere*, **8**, 453–470, doi:10.5194/tc-8-453-2014.
- Gregory, J. M., P. a. Stott, D. J. Cresswell, N. a. Rayner, C. Gordon, and D. M. H. Sexton, 2002: Recent and future changes in Arctic sea ice simulated by the HadCM3 AOGCM. *Geophysical Research Letters*, **29** (24), 1999–2002, doi:10.1029/2001GL014575.
- Hansen, J., R. Ruedy, M. Sato, and K. Lo, 2010: Global surface temperature change. *Rev. Geophys.*, **48** (4), RG4004, doi:10.1029/2010RG000345.1.INTRODUCTION.
- Haumann, F. A., D. Notz, and H. Schmidt, 2014: Anthropogenic influence on recent circulation-driven Antarctic sea ice changes. *Geophysical Research Letters*, **41** (23), 8429–8437, doi:10.1002/2014GL061659, URL <http://doi.wiley.com/10.1002/2014GL061659>.
- Holland, M. M., C. M. Bitz, L.-B. Tremblay, and D. A. Bailey, 2008: The Role of Natural Versus Forced Change in Future Rapid Summer Arctic Ice Loss. *Arctic Sea Ice Decline: Observations, Projections, Mechanisms, and Implications*, Vol. 3, 133–150, doi:10.1029/180GM10.
- Ice, S., and Coauthors, 2015: Recent changes in Antarctic Subject Areas : Author for correspondence :.
- IPCC, 2007: *Climate Change 2007: The Physical Science Basis. Contribution of Working Group I to the Fourth Assessment Report of the Intergovernmental Panel on Climate Change*. Cambridge University Press, Cambridge, UK, 996 pp.
- IPCC, 2013: *Climate Change 2013: The Physical Science Basis. Contribution of Working Group I to the Fifth Assessment Report of the Intergovernmental Panel on Climate Change*. Cambridge University Press, Cambridge, UK, 1535 pp.
- Jahn, A., and Coauthors, 2012: Late-twentieth-century simulation of arctic sea ice and ocean properties in the CCSM4. *Journal of Climate*, **25** (5), 1431–1452, doi:10.1175/JCLI-D-11-00201.1.
- Karl, T. R., and Coauthors, 2015: Possible artifacts of data biases in the recent global surface warming hiatus. *Science*, **4** (June), 1–7.
- Kay, J. E., C. Deser, and A. S. Phillips, 2014: The Community Earth System Model (CESM) Large Ensemble Project: A Community Resource for Studying Climate Change in the Presence of Internal Climate Variability. *Bulletin of the American Meteorological Society*, doi:10.1175/BAMS-D-14-00017.1.
- Kay, J. E., M. M. Holland, and A. Jahn, 2011: Inter-annual to multi-decadal Arctic sea ice extent trends in a warming world. *Geophysical Research Letters*, **38** (15), n/a–n/a, doi:10.1029/2011GL048008.
- Kosaka, Y., and S.-P. Xie, 2013: Recent global-warming hiatus tied to equatorial Pacific surface cooling. *Nature*, **501** (7467), 403–407, doi:10.1038/nature12534, URL <http://www.nature.com/doi/10.1038/nature12534>.
- Mahlstein, I., P. R. Gent, and S. Solomon, 2013: Historical Antarctic mean sea ice area, sea ice trends, and winds in CMIP5 simulations. *Journal of Geophysical Research: Atmospheres*, **118** (11), 5105–5110, doi:10.1002/jgrd.50443.
- Mahlstein, I., and R. Knutti, 2012: September Arctic sea ice predicted to disappear near 2C global warming above present. *Journal of Geophysical Research*, **117** (D6), D06 104, doi:10.1029/2011JD016709.
- Meehl, G. a., C. Covey, T. Delworth, M. Latif, B. McAvaney, J. F. B. Mitchell, R. J. Stouffer, and K. E. Taylor, 2007: The WCRP CMIP3 multimodel dataset: A new era in climatic change research. *Bulletin of the American Meteorological Society*, **88** (9), 1383–1394, doi:10.1175/BAMS-88-9-1383.
- Notz, D., 2014: Sea-ice extent and its trend provide limited metrics of model performance. *The Cryosphere*, **8** (1), 229–243, doi:10.5194/tc-8-229-2014.
- Polvani, L. M., and K. L. Smith, 2013: Can natural variability explain observed Antarctic sea ice trends? New modeling evidence from CMIP5. *Geophysical Research Letters*, **40** (12), 3195–3199, doi:10.1002/grl.50578.

- Purich, A., W. Cai, M. H. England, and T. Cowan, 2016: Evidence for link between modelled trends in Antarctic sea ice and underestimated westerly wind changes. *Nature Communications*, **7** (May 2015), 10 409, doi:10.1038/ncomms10409, URL <http://www.nature.com/doi/10.1038/ncomms10409>.
- Rampal, P., J. Weiss, C. Dubois, and J. M. Campin, 2011: IPCC climate models do not capture Arctic sea ice drift acceleration: Consequences in terms of projected sea ice thinning and decline. *Journal of Geophysical Research: Oceans*, **116** (9), 1–17, doi:10.1029/2011JC007110.
- Rosenblum, E., and I. Eisenman, 2016: Apparent arctic sea ice modeling improvement caused by volcanoes. *Journal of Climate*, *Submitted*.
- Santer, B. D., and Coauthors, 2008: Consistency of modelled and observed temperature trends in the tropical troposphere. *International Journal of Climatology*, **28** (13), 1703–1722, doi:10.1002/joc.1756, URL <http://www3.interscience.wiley.com/journal/4735/homehttp://doi.wiley.com/10.1002/joc.1756>.
- Screen, J. A., 2011: Sudden increase in Antarctic sea ice: Fact or artifact? *Geophys. Res. Lett.*, **38**, L13 702, doi:10.1029/2011GL047553.
- Stroeve, J., M. M. Holland, W. Meier, T. Scambos, and M. Serreze, 2007: Arctic sea ice decline: Faster than forecast. *Geophysical Research Letters*, **34** (9), L09 501, doi:10.1029/2007GL029703.
- Stroeve, J., and D. Notz, 2015: Insights on past and future sea-ice evolution from combining observations and models. *Global and Planetary Change*, doi:10.1016/j.gloplacha.2015.10.011, URL <http://linkinghub.elsevier.com/retrieve/pii/S092181811530093X>.
- Stroeve, J. C., V. Kattsov, A. Barrett, M. Serreze, T. Pavlova, M. Holland, and W. N. Meier, 2012: Trends in Arctic sea ice extent from CMIP5, CMIP3 and observations. *Geophysical Research Letters*, **39** (16), n/a–n/a, doi:10.1029/2012GL052676.
- Swart, N. C., and J. C. Fyfe, 2013: The influence of recent Antarctic ice sheet retreat on simulated sea ice area trends. *Geophysical Research Letters*, **40** (August), 4328–4332, doi:10.1002/grl.50820.
- Swart, N. C., J. C. Fyfe, E. Hawkins, J. E. Kay, and A. Jahn, 2015: Influence of internal variability on Arctic sea-ice trends. *Nature Publishing Group*, **5** (2), 86–89, doi:10.1038/nclimate2483.
- Taylor, K. E., R. J. Stouffer, and G. A. Meehl, 2011: An overview of CMIP5 and the experiment design. *Bull. Amer. Meteor. Soc.*, **93** (4), 485–498, doi:10.1175/BAMS-D-11-00094.1.
- Turner, J., T. J. Bracegirdle, T. Phillips, G. J. Marshall, and J. S. Hosking, 2013: An Initial Assessment of Antarctic Sea Ice Extent in the CMIP5 Models. *Journal of Climate*, **26** (5), 1473–1484, doi:10.1175/JCLI-D-12-00068.1.
- Uotila, P., P. Holland, T. Vihma, S. Marsland, and N. Kimura, 2014: Is realistic Antarctic sea ice extent in climate models the result of excessive ice drift? *Ocean Modelling*, doi:10.1016/j.ocemod.2014.04.004.
- Wettstein, J. J., and C. Deser, 2014: Internal Variability in Projections of Twenty-First-Century Arctic Sea Ice Loss: Role of the Large-Scale Atmospheric Circulation. *Journal of Climate*, **27** (2), 527–550, doi:10.1175/JCLI-D-12-00839.1, URL <http://journals.ametsoc.org/doi/abs/10.1175/JCLI-D-12-00839.1>.
- Winton, M., 2011: Do Climate Models Underestimate the Sensitivity of Northern Hemisphere Sea Ice Cover? *Journal of Climate*, **24** (15), 3924–3934, doi:10.1175/2011JCLI4146.1.
- Xie, S.-P., Y. Kosaka, and Y. M. Okumura, 2016: Distinct energy budgets for anthropogenic and natural changes during global warming hiatus. *Nature Geoscience*, **9** (January), 29–33, doi:10.1038/ngeo2581.
- Zunz, V., H. Goosse, and F. Massonnet, 2013: How does internal variability influence the ability of CMIP5 models to reproduce the recent trend in Southern Ocean sea ice extent? *The Cryosphere*, **7** (2), 451–468, doi:10.5194/tc-7-451-2013.

	Arctic	Antarctic
1979-2013 Trends	16/100 (16%)	3/100 (3.0%)
1979-2013 Effective Trends	0/100 (0%)	0/100 (0%)
Pseudo-ensemble	1/1251 (0.078%)	39/1275 (2.6%)

TABLE 1. Fraction of simulated Arctic sea ice trends that are as extreme as the observations using the distribution of CMIP5 simulated trends, effective trends (see Section 5), and a pseudo-ensemble of 35-year periods that have similar levels of global warming to the observations (see Section 6). The first column is the fraction with Arctic sea ice retreat as rapid as the observations, and the second column is the fraction with Antarctic sea ice expansion as rapid as the observations. There are 100 simulations of 1979-2013 in the CMIP5 ensemble analyzed here and 1275 overlapping 35-year periods in the pseudo-ensemble. Percentages are indicated to aid in comparison between the rows.

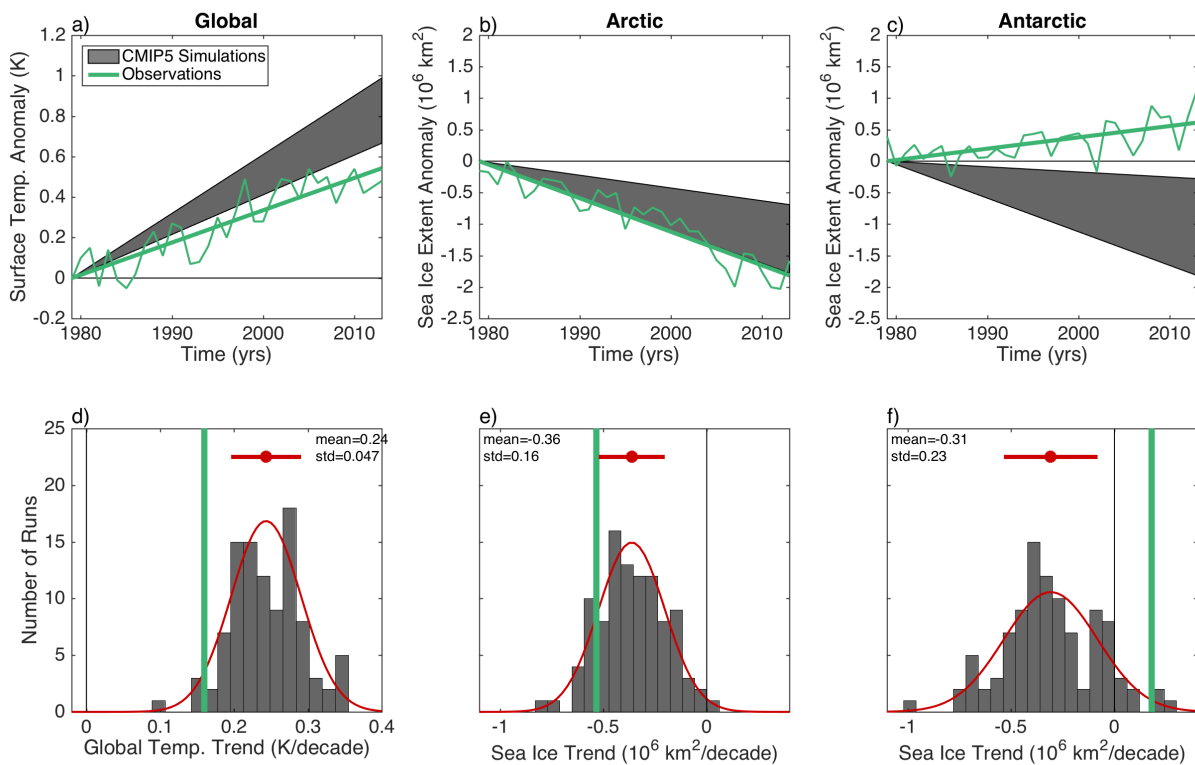


FIG. 1. Observed and CMIP5 modeled annual-mean (a) global-mean surface temperature, (b) Arctic, and (c) Antarctic sea ice extent. Anomalies from 1979 and resulting time trend are indicated for observations (green), and shadings indicate one standard deviation among the models around the CMIP5 ensemble-mean trend. (d-f) Accompanying histograms show the corresponding distribution of (d) global-mean surface temperature, (e) Arctic, and (f) Antarctic sea ice extent trends from the 100 CMIP5 simulations, with the observed trend indicated by a green line in each panel. Standard deviations of the distribution around the CMIP5 ensemble-mean are also shown in red.

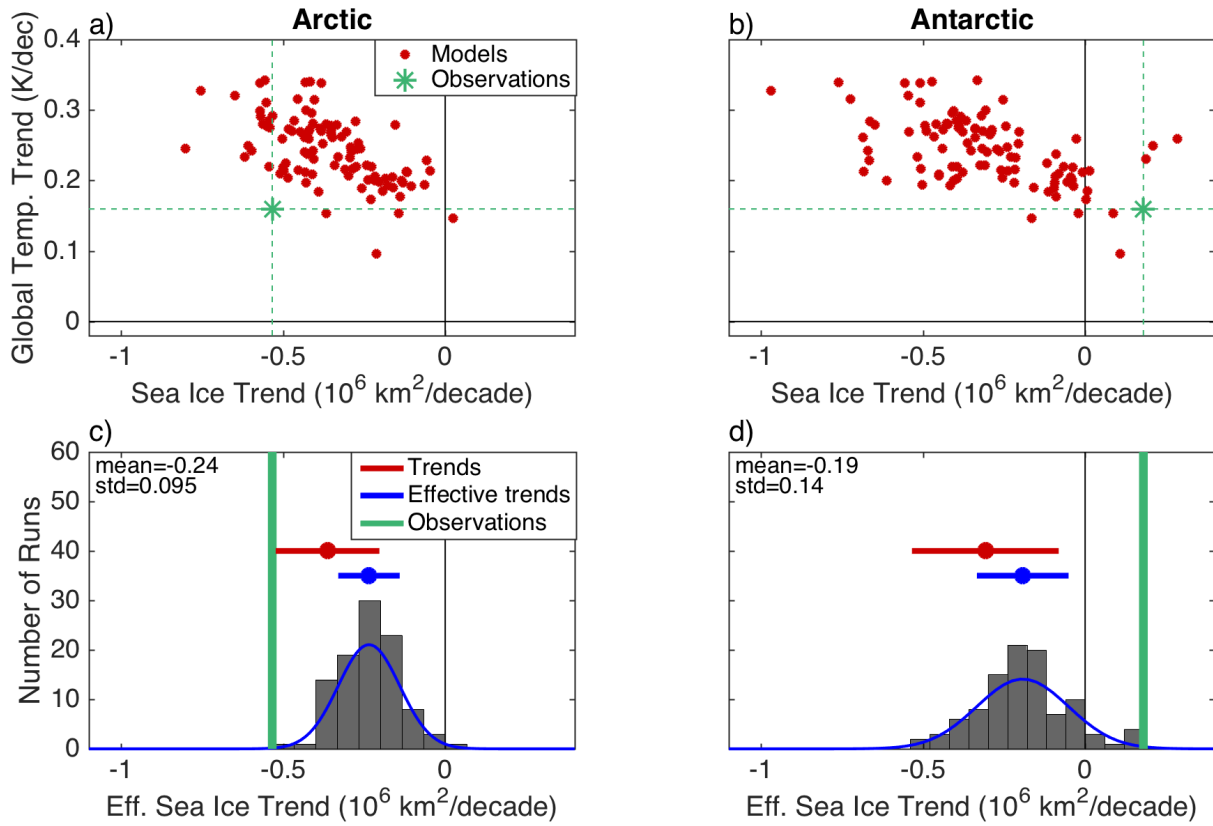


FIG. 2. Observed and CMIP5 simulated annual-mean global-mean surface temperature trends plotted versus the corresponding (a) Arctic and (b) Antarctic sea ice trends compared to the observed trends (dashed lines). (e-f) Distribution of simulated effective sea ice trends (see text for details) from each CMIP5 simulation, with the observed trend indicated by a green line. Standard deviations from the distribution simulated sea ice trends (red, from Figures 1e-f) and effective sea ice trends (blue) are also shown.

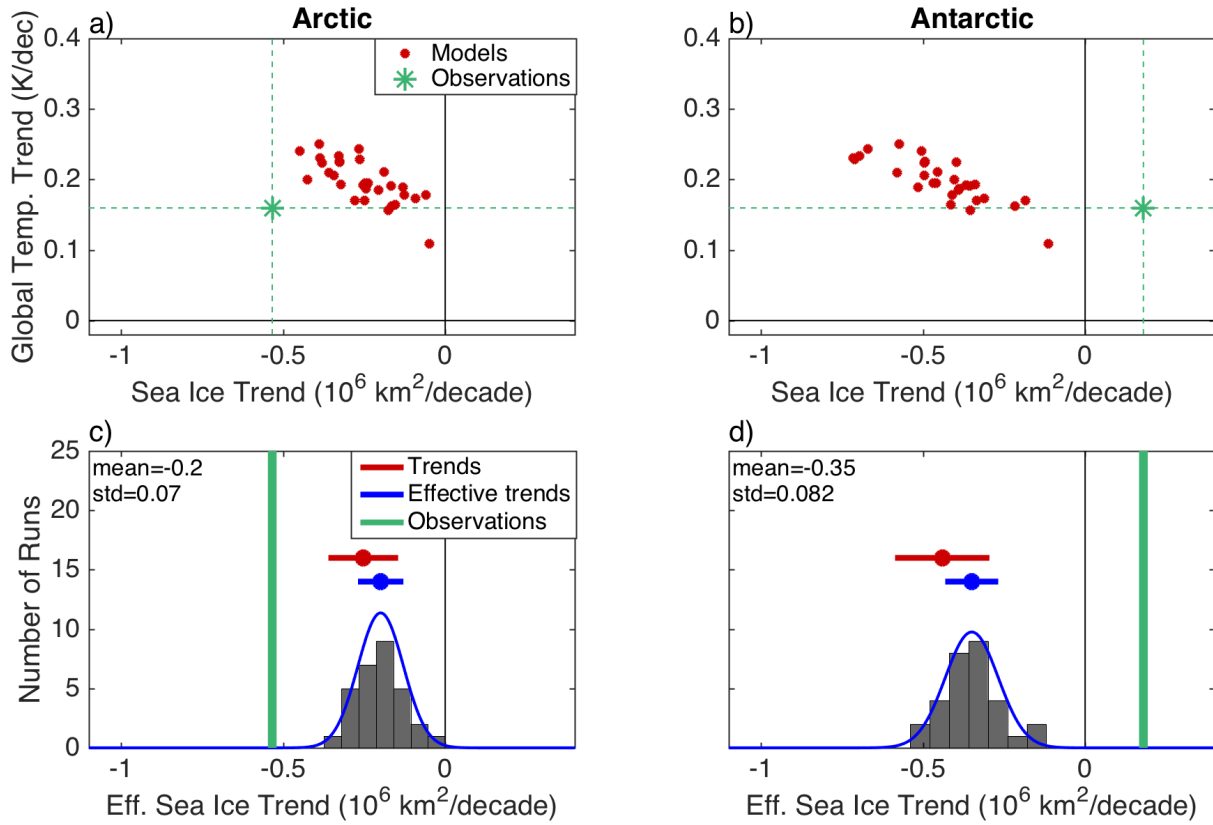


FIG. 3. As in Figure 2, but using CESM-LE simulations instead of CMIP5.

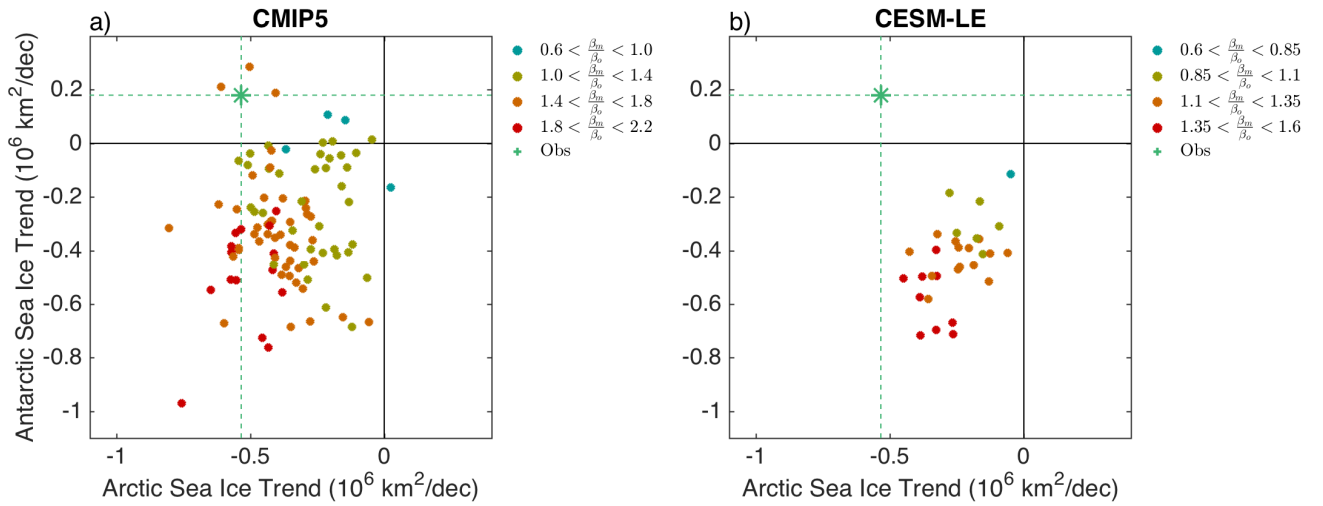


FIG. 4. Observed and simulated annual-mean Antarctic sea ice trends versus the corresponding Arctic sea ice trends using (a) CMIP5 models and (b) CESM-LE simulations. Dashed lines represent the observed trends, and the color of each simulation indicates the ratio between the simulated (β_m) and observed (β_o) values of the annual-mean global-mean surface temperature trend.

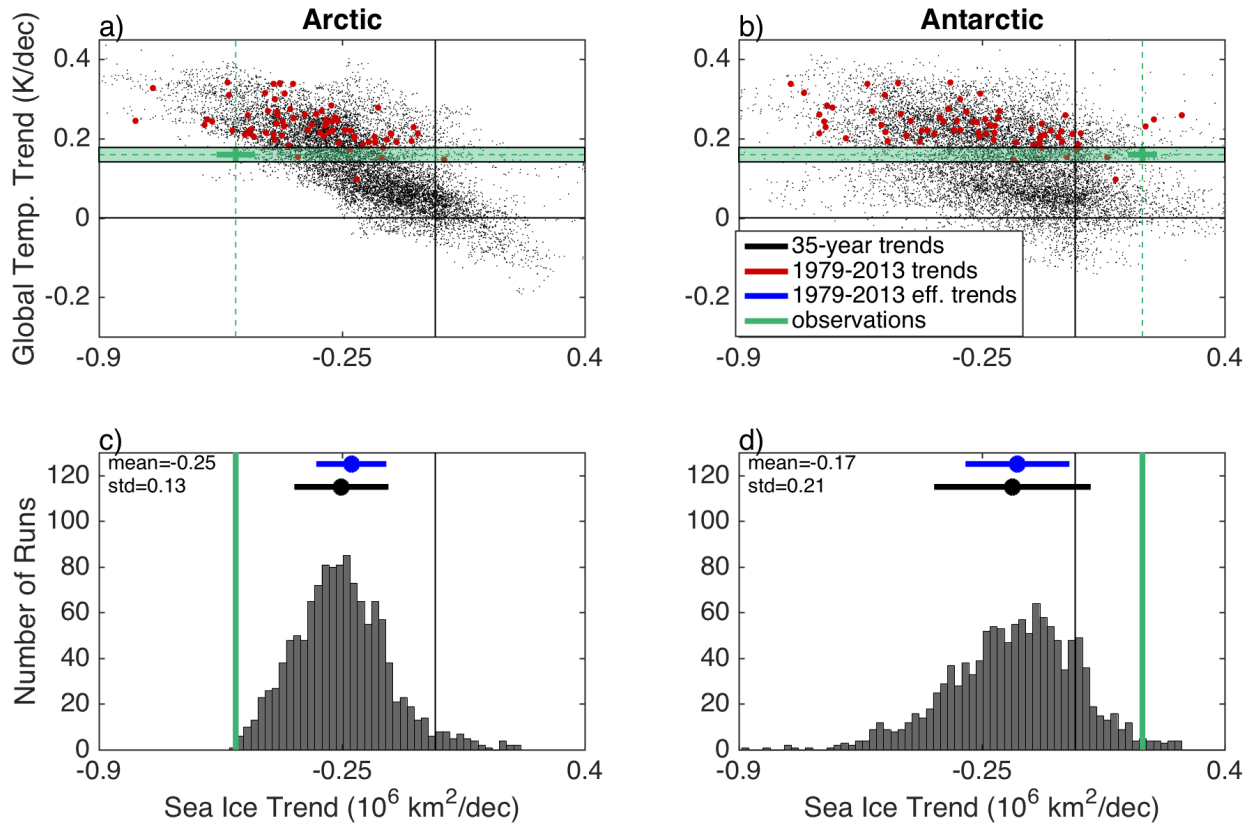


FIG. 5. Observed and simulated annual-mean (a) Arctic sea ice trends and (b) Antarctic sea ice trends versus the global-mean surface temperature trends from all overlapping 35-year periods in 73 CMIP5 simulations of 1900-2100 are plotted (12,024 points in total), 1979-2013 trends are also indicated in red (as in Figure 2a-b). Green lines represent the observed trends, and cross represents the 1-sigma confidence interval. Global-mean surface temperature trends that are within one standard deviation of the observed trend are highlighted in green. Sea ice trends associated with the highlighted regions are shown in histograms below (c,d), with the observed trend indicated by a thick green line. Standard deviations of this distribution (black) and the distribution of 1979-2013 effective sea ice trends (blue, as in Figure 3c-d) are also shown. As in Figure 4, but using 73 CMIP5 simulations of 1900-2100.

Supplemental Material for “Can natural variability explain the discrepancy between observed and modeled sea ice trends?”

ERICA ROSENBLUM AND IAN EISENMAN

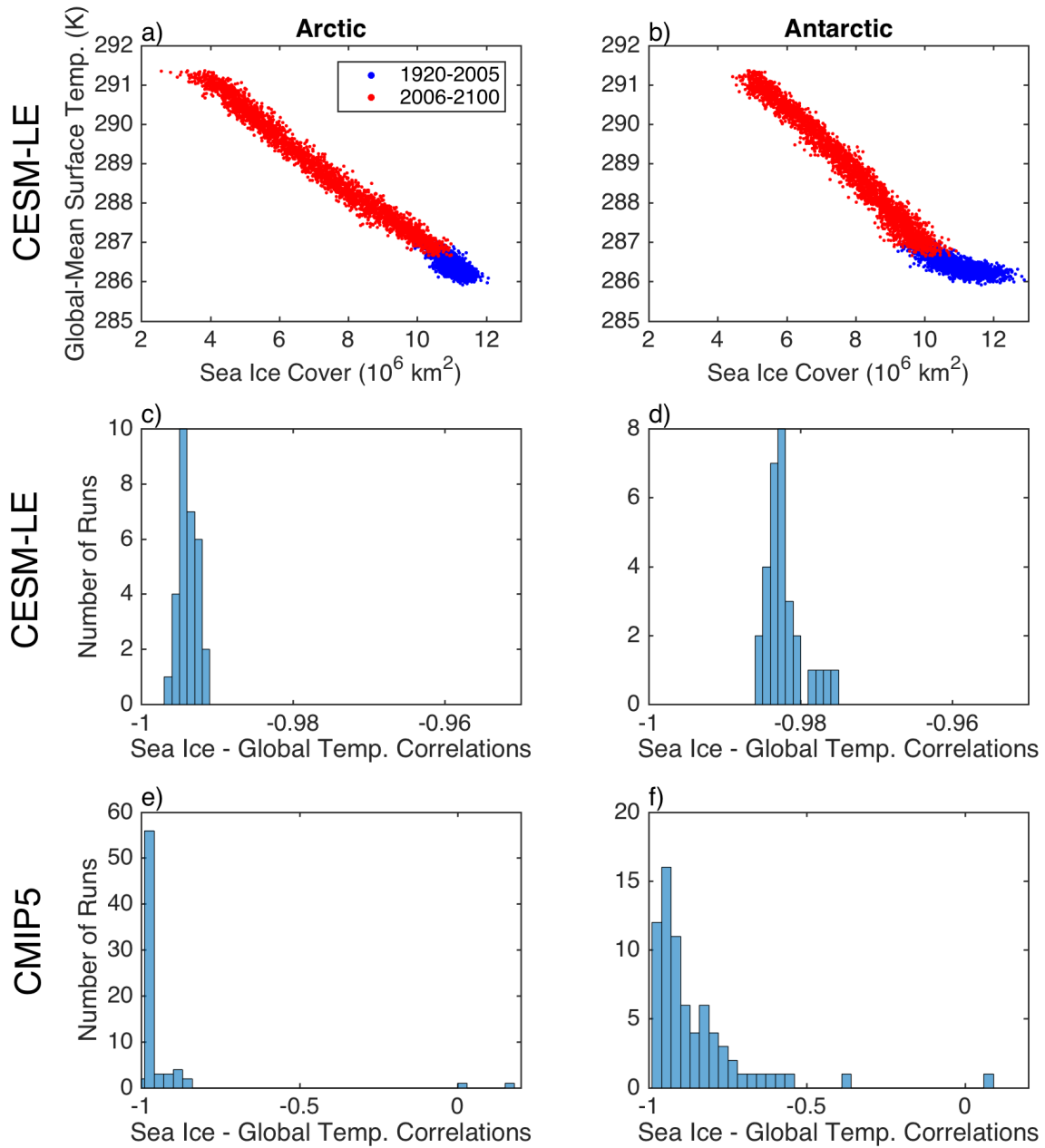


FIG. S1. Annual global-mean surface air temperature versus the (a) Arctic and (b) Antarctic sea ice extent using 30 CSM-LE simulations of 1920-2100. Years associated with 1920-2005 and 2006-2100 are also indicated. Histogram of the correlations between (c,e) Arctic sea ice cover and (d,f) Antarctic sea ice extent with the global-mean surface air temperature from each (c-d) CSM-LE simulation of 1920-2100 and (e-f) CMIP5 simulation of 1900-2100.

arXiv:1606.08519v1 [physics.ao-ph] 28 Jun 2016

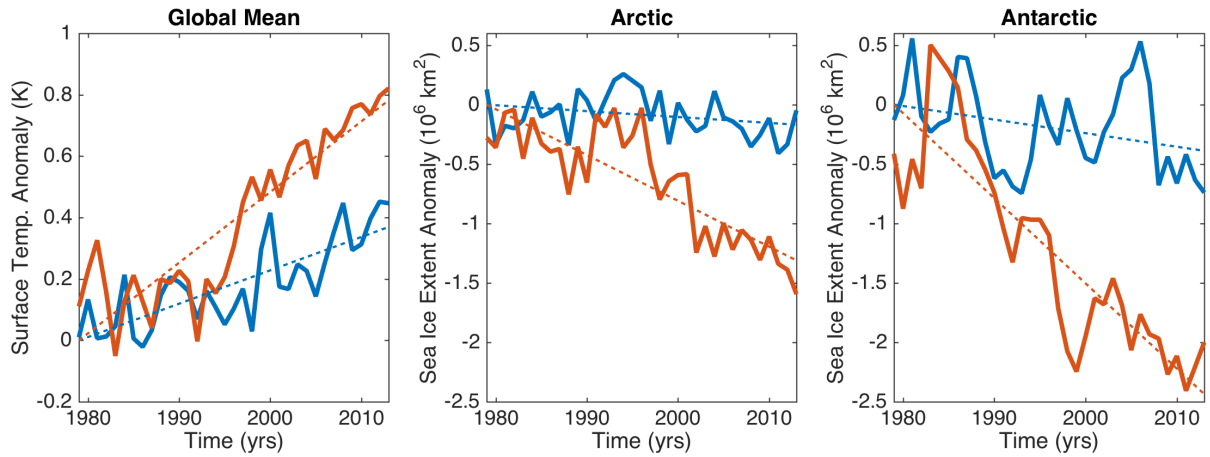


FIG. S2. Time series of annual (a) global-mean surface air temperature, (b) Arctic sea ice extent, and (c) Antarctic sea ice extent and corresponding trends from two CESM-LE simulations.

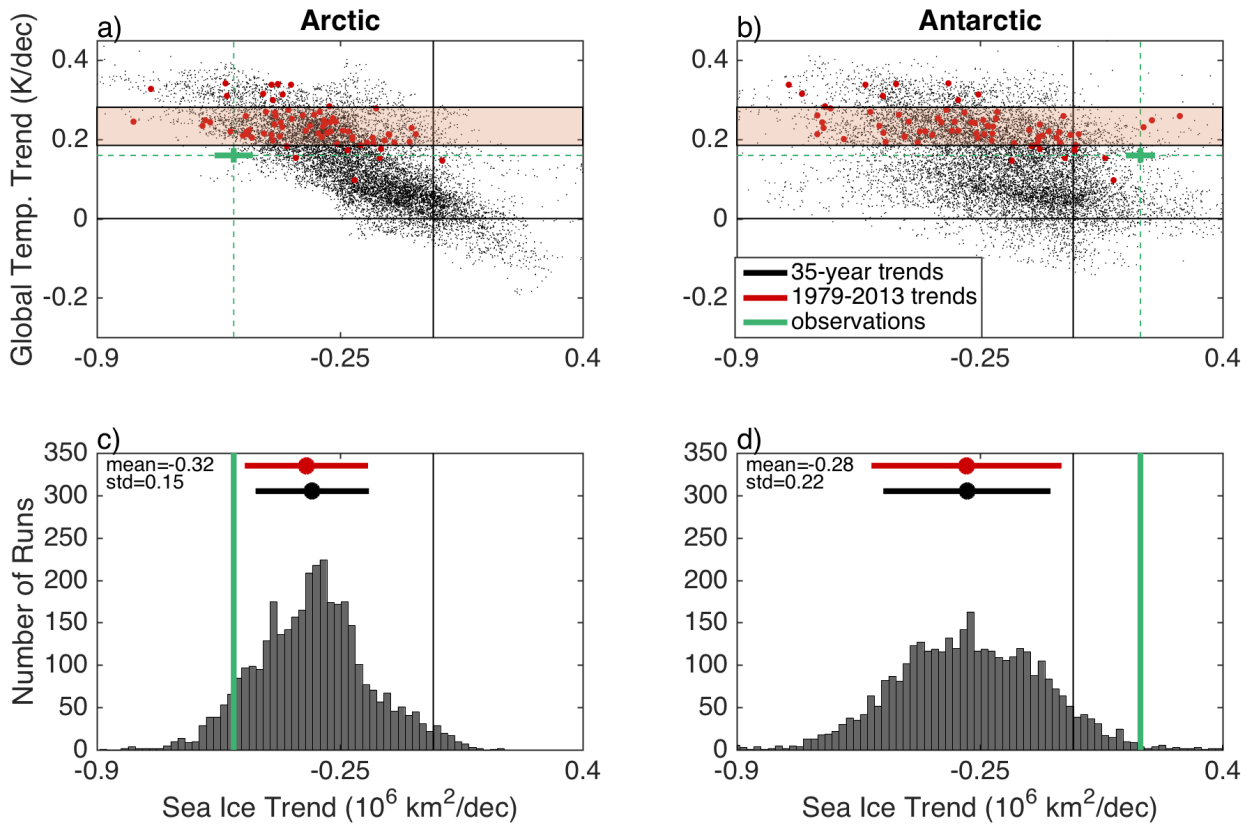


FIG. S3. (a-b) As in Figure 5a-b, but here the red highlighted region indicates all 35-year global-mean surface air temperature trends that are within one standard deviation of the 1979-2013 CMIP5 ensemble mean (Figure 1d). Sea ice trends associated with the highlighted regions are shown in the histograms below (c,d), with the observed trend indicated by a thick green line. Standard deviations of this distribution (black) and the distribution of 1979-2013 sea ice trends (red) are also shown.

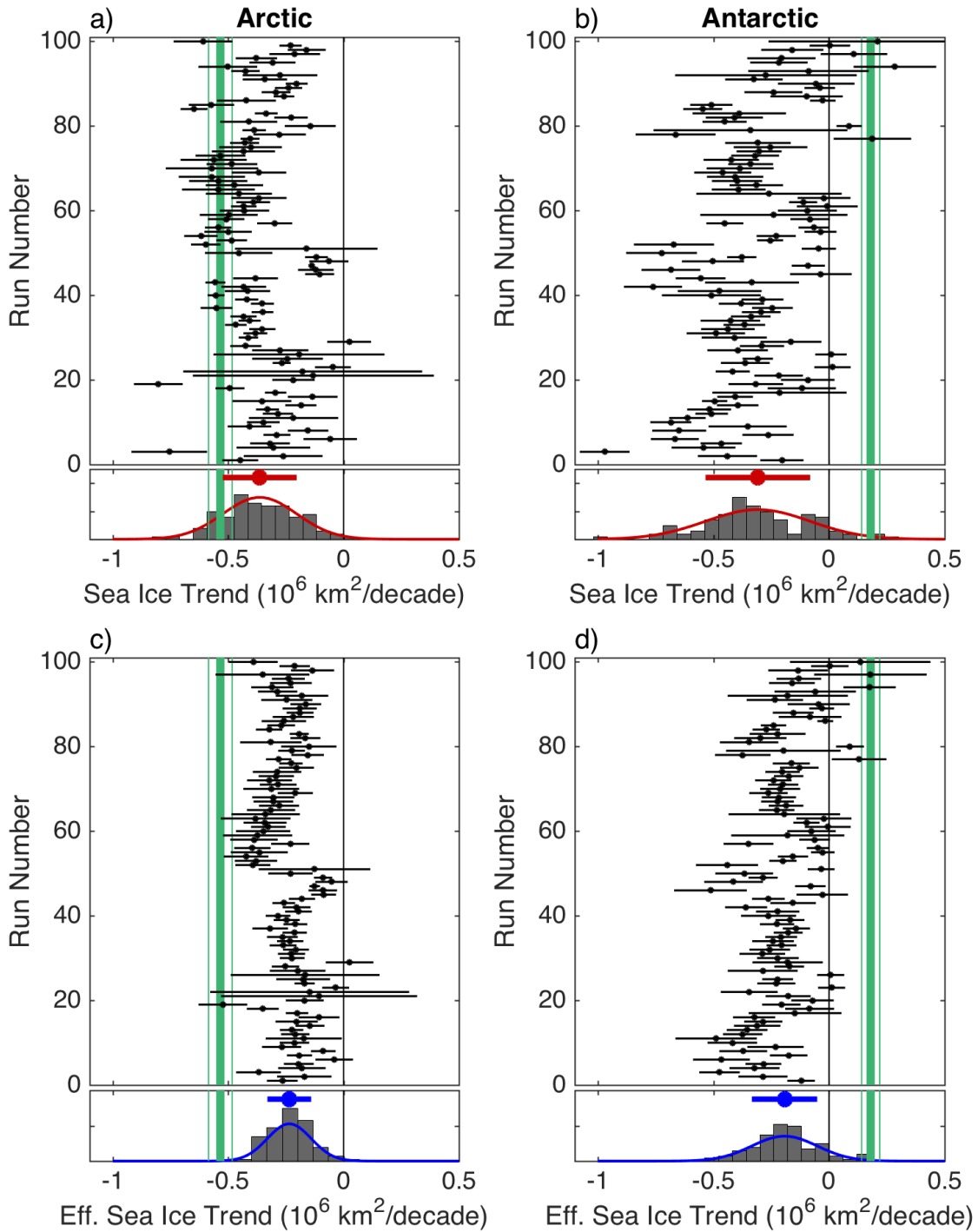


FIG. S4. Distribution of 100 CMIP5 simulated 1979–2013 (a,c) Arctic and (b,d) Antarctic (a–b) sea ice trends and (c–d) effective sea ice trends, as in Figures 1e–f and 2c–d. Above each distribution, the mean and 1-sigma confidence interval of each simulated 35-year trend is indicated (see text for details). The observed trend is indicated by a thick green line, surrounded by thin lines that indicate the 1-sigma confidence interval.

Model	Run	Temp	Arctic	Antarctic	Eff_Arctic	Eff_Antarctic
observations	0	0.160	-0.534	0.180	-0.534	0.180
ACCESS1-0	1	0.269	-0.448	-0.204	-0.266	-0.121
ACCESS1-3	1	0.245	-0.262	-0.440	-0.170	-0.286
BCC-CSM1-1	1	0.249	-0.609	0.210	-0.391	0.135
BNU-ESM	1	0.327	-0.755	-0.971	-0.369	-0.474
CCSM4	1	0.269	-0.304	-0.543	-0.181	-0.323
CCSM4	2	0.262	-0.319	-0.466	-0.194	-0.284
CCSM4	3	0.229	-0.058	-0.667	-0.040	-0.466
CCSM4	4	0.241	-0.289	-0.264	-0.191	-0.175
CCSM4	5	0.279	-0.154	-0.648	-0.088	-0.371
CCSM4	6	0.243	-0.408	-0.352	-0.268	-0.232
CESM1-BGC	1	0.261	-0.348	-0.685	-0.213	-0.418
CESM1-CAM5	1	0.200	-0.217	-0.613	-0.173	-0.489
CESM1-CAM5	2	0.217	-0.284	-0.508	-0.209	-0.374
CESM1-CAM5	3	0.234	-0.330	-0.519	-0.225	-0.355
CESM1-WACCM	2	0.203	-0.185	-0.395	-0.146	-0.311
CESM1-WACCM	3	0.278	-0.354	-0.495	-0.203	-0.285
CESM1-WACCM	4	0.200	-0.134	-0.406	-0.107	-0.324
CMCC-CMS	1	0.233	-0.295	-0.215	-0.202	-0.147
CMCC-CM	1	0.224	-0.492	-0.118	-0.350	-0.084
CNRM-CM5	1	0.245	-0.803	-0.317	-0.523	-0.206
CSIRO-Mk3-6-0	10	0.206	-0.217	-0.092	-0.168	-0.071
CSIRO-Mk3-6-0	1	0.197	-0.131	-0.218	-0.106	-0.177
CSIRO-Mk3-6-0	2	0.193	-0.177	-0.417	-0.147	-0.345
CSIRO-Mk3-6-0	3	0.214	-0.046	0.015	-0.034	0.011
CSIRO-Mk3-6-0	4	0.254	-0.268	-0.362	-0.169	-0.228
CSIRO-Mk3-6-0	5	0.221	-0.243	-0.308	-0.175	-0.222
CSIRO-Mk3-6-0	6	0.185	-0.194	0.008	-0.167	0.007
CSIRO-Mk3-6-0	7	0.220	-0.274	-0.395	-0.199	-0.287
CSIRO-Mk3-6-0	8	0.268	-0.424	-0.290	-0.252	-0.173

continued on next page ...

Model	Run	Temp	Arctic	Antarctic	Eff_Arctic	Eff_Antarctic
CSIRO-Mk3-6-0	9	0.147	0.024	-0.165	0.026	-0.179
CanCM4	10	0.296	-0.412	-0.410	-0.223	-0.221
CanCM4	1	0.270	-0.382	-0.490	-0.226	-0.289
CanCM4	2	0.272	-0.352	-0.438	-0.206	-0.257
CanCM4	3	0.284	-0.467	-0.367	-0.262	-0.206
CanCM4	4	0.281	-0.407	-0.427	-0.231	-0.242
CanCM4	5	0.261	-0.434	-0.339	-0.265	-0.207
CanCM4	6	0.265	-0.351	-0.293	-0.212	-0.177
CanCM4	7	0.277	-0.551	-0.245	-0.318	-0.141
CanCM4	8	0.269	-0.352	-0.379	-0.209	-0.225
CanCM4	9	0.272	-0.420	-0.288	-0.246	-0.169
CanESM2	1	0.311	-0.553	-0.510	-0.284	-0.262
CanESM2	2	0.340	-0.416	-0.473	-0.195	-0.222
CanESM2	3	0.339	-0.433	-0.762	-0.204	-0.359
CanESM2	4	0.342	-0.556	-0.333	-0.259	-0.156
CanESM2	5	0.338	-0.381	-0.556	-0.180	-0.263
EC-EARTH	7	0.192	-0.104	-0.035	-0.087	-0.030
EC-EARTH	8	0.213	-0.120	-0.684	-0.090	-0.513
FGOALS-g2	1	0.177	-0.139	-0.090	-0.126	-0.081
FIO-ESM	1	0.194	-0.064	-0.502	-0.052	-0.413
FIO-ESM	3	0.211	-0.118	-0.378	-0.089	-0.285
GFDL-CM3	1	0.315	-0.455	-0.725	-0.230	-0.367
GFDL-ESM2G	1	0.260	-0.471	0.333	-0.290	0.205
GFDL-ESM2M	1	0.205	-0.162	-0.044	-0.126	-0.034
GISS-E2-H-CC	1	0.243	-0.597	-0.671	-0.393	-0.442
GISS-E2-H	1	0.204	-0.485	-0.255	-0.380	-0.200
GISS-E2-H	2	0.234	-0.618	-0.229	-0.422	-0.156
GISS-E2-H	3	0.219	-0.500	-0.037	-0.365	-0.027
GISS-E2-H	4	0.220	-0.544	-0.066	-0.395	-0.048
GISS-E2-H	5	0.206	-0.299	-0.451	-0.231	-0.349

continued on next page ...

Model	Run	Temp	Arctic	Antarctic	Eff_Arctic	Eff_Antarctic
GISS-E2-R-CC	1	0.209	-0.509	-0.082	-0.388	-0.062
GISS-E2-R	1	0.213	-0.498	-0.239	-0.372	-0.179
GISS-E2-R	2	0.197	-0.429	-0.094	-0.349	-0.076
GISS-E2-R	3	0.212	-0.432	-0.008	-0.326	-0.006
GISS-E2-R	4	0.184	-0.392	-0.112	-0.340	-0.098
GISS-E2-R	5	0.154	-0.367	-0.022	-0.381	-0.022
GISS-E2-R	6	0.214	-0.454	-0.260	-0.338	-0.193
HadCM3	10	0.275	-0.543	-0.391	-0.314	-0.227
HadCM3	1	0.270	-0.473	-0.315	-0.280	-0.186
HadCM3	2	0.285	-0.543	-0.398	-0.304	-0.223
HadCM3	3	0.299	-0.571	-0.406	-0.305	-0.217
HadCM3	4	0.280	-0.367	-0.460	-0.209	-0.262
HadCM3	5	0.290	-0.570	-0.385	-0.313	-0.211
HadCM3	6	0.273	-0.484	-0.339	-0.283	-0.199
HadCM3	7	0.280	-0.563	-0.423	-0.321	-0.241
HadCM3	8	0.292	-0.533	-0.320	-0.291	-0.175
HadCM3	9	0.240	-0.434	-0.303	-0.288	-0.201
IPSL-CM5A-LR	1	0.314	-0.403	-0.253	-0.205	-0.129
IPSL-CM5A-LR	2	0.300	-0.429	-0.308	-0.228	-0.164
IPSL-CM5A-LR	3	0.230	-0.405	0.188	-0.281	0.130
IPSL-CM5A-LR	4	0.284	-0.277	-0.664	-0.156	-0.373
IPSL-CM5A-MR	1	0.274	-0.387	-0.340	-0.225	-0.198
IPSL-CM5B-LR	1	0.153	-0.144	0.087	-0.151	0.090
MIROC-ESM-CHEM	1	0.208	-0.411	-0.452	-0.315	-0.346
MIROC-ESM	1	0.220	-0.228	-0.410	-0.165	-0.297
MIROC4h	1	0.279	-0.335	-0.388	-0.192	-0.223
MIROC4h	2	0.321	-0.648	-0.546	-0.323	-0.272
MIROC4h	3	0.338	-0.573	-0.509	-0.270	-0.240
MIROC5	1	0.260	-0.421	-0.027	-0.259	-0.017
MIROC5	2	0.189	-0.258	-0.097	-0.218	-0.082

continued on next page ...

Model	Run	Temp	Arctic	Antarctic	Eff_Arctic	Eff_Antarctic
MIROC5	3	0.248	-0.292	-0.241	-0.188	-0.155
MIROC5	4	0.200	-0.239	-0.040	-0.190	-0.032
MIROC5	5	0.198	-0.203	-0.056	-0.164	-0.045
MPI-ESM-LR	1	0.221	-0.341	-0.325	-0.246	-0.235
MPI-ESM-LR	2	0.244	-0.275	-0.273	-0.180	-0.179
MPI-ESM-LR	3	0.237	-0.425	-0.089	-0.286	-0.060
MPI-ESM-MR	1	0.259	-0.502	0.285	-0.309	0.175
MPI-ESM-MR	2	0.215	-0.308	-0.217	-0.228	-0.161
MPI-ESM-MR	3	0.252	-0.378	-0.206	-0.239	-0.131
MRI-CGCM3	1	0.096	-0.212	0.108	-0.351	0.179
NorESM1-ME	1	0.190	-0.160	-0.159	-0.134	-0.134
NorESM1-M	1	0.173	-0.230	0.004	-0.212	0.003
CESM-LE	1	0.199	-0.426	-0.404	-0.341	-0.323
CESM-LE	2	0.226	-0.326	-0.495	-0.230	-0.349
CESM-LE	3	0.195	-0.239	-0.461	-0.195	-0.377
CESM-LE	4	0.170	-0.278	-0.185	-0.261	-0.174
CESM-LE	5	0.170	-0.250	-0.335	-0.234	-0.314
CESM-LE	6	0.224	-0.326	-0.397	-0.232	-0.282
CESM-LE	7	0.193	-0.323	-0.339	-0.268	-0.281
CESM-LE	8	0.223	-0.380	-0.497	-0.272	-0.355
CESM-LE	9	0.228	-0.264	-0.711	-0.184	-0.498
CESM-LE	10	0.185	-0.206	-0.391	-0.177	-0.336
CESM-LE	11	0.210	-0.358	-0.581	-0.272	-0.443
CESM-LE	12	0.243	-0.267	-0.670	-0.175	-0.440
CESM-LE	13	0.250	-0.389	-0.574	-0.248	-0.366
CESM-LE	14	0.191	-0.168	-0.356	-0.140	-0.298
CESM-LE	15	0.187	-0.244	-0.389	-0.208	-0.332
CESM-LE	16	0.189	-0.131	-0.515	-0.111	-0.435
CESM-LE	17	0.210	-0.188	-0.455	-0.142	-0.345
CESM-LE	18	0.230	-0.386	-0.716	-0.268	-0.497

continued on next page ...

Model	Run	Temp	Arctic	Antarctic	Eff_Arctic	Eff_Antarctic
CESM-LE	19	0.240	-0.450	-0.505	-0.299	-0.335
CESM-LE	20	0.233	-0.328	-0.697	-0.225	-0.477
CESM-LE	21	0.162	-0.164	-0.218	-0.162	-0.214
CESM-LE	22	0.205	-0.343	-0.495	-0.266	-0.385
CESM-LE	23	0.174	-0.092	-0.310	-0.084	-0.285
CESM-LE	24	0.192	-0.254	-0.367	-0.211	-0.305
CESM-LE	25	0.164	-0.154	-0.414	-0.150	-0.402
CESM-LE	26	0.195	-0.246	-0.469	-0.202	-0.384
CESM-LE	27	0.178	-0.059	-0.409	-0.053	-0.367
CESM-LE	28	0.109	-0.050	-0.114	-0.073	-0.168
CESM-LE	29	0.157	-0.175	-0.355	-0.179	-0.362
CESM-LE	30	0.178	-0.127	-0.410	-0.114	-0.367

TABLE S1. Trends in CMIP5 and CESM-LE simulations (note that table spans the preceding pages). Units are 10^6 km²/decade. See <http://cmip-pcmdi.llnl.gov/cmip5> for a list of the modeling centers associated with each model listed here. Note that one simulation (CSIRO-Mk3-6-0 run9) has an Arctic sea ice trend that is nearly zero, which is the apparently coincidental result of a series of large increases and decreases in the simulated sea ice cover.